공학석사학위논문

A Study on the Design of Electric Pump for Small Liquid-Methane Rocket Engine

소형 액체메탄 로켓엔진을 위한 전기펌프 설계에 대한 고찰

2020 년 2 월

서울대학교 대학원

기계항공공학부

윤 준 태

소형 액체메탄 로켓엔진을 위한 전기펌프 설계에 대한 고찰

A Study on the Design of Electric Pump for Small Liquid-Methane Rocket Engine

지도교수 윤 영 빈

이 논문을 공학석사 학위논문으로 제출함

2019 년 12 월

서울대학교 대학원
기계항공공학부
윤 준 태

윤준태의 공학석사 학위논문을 인준함

2019 년 12 월

위 원 장 _____

부위원장 _____

위 원 _____

Abstract

A Study on the Design of Electric Pump for Small Liquid-Methane Rocket Engine

Juntae Yoon
School of Mechanical and Aerospace Engineering
The Graduate School
Seoul National University

Due to the Fourth Industrial Revolution, the demand for small satellites is greatly increasing, and the market for small launch vehicles for efficiently launching these small satellites is growing rapidly. However, since the turbopump system, which is used for the existing large launch vehicle, has a complicated configuration and a high manufacturing and operating cost, the electric pump system has attracted attention as a substitute for a small launch vehicle instead of the turbopump. In particular, due to the rapid development of battery technology, the development of a light and energy-dense battery

has made it possible to apply an electric pump system that is more efficient and cheaper than a turbopump for a small rocket engine. However, recent small launch vehicles are mostly having a thrust of 1 ton or more and are not suitable for launching nanosatellites, which are rapidly increasing in demand recently. So, through this study, an electric pump for driving 5,000 Newton-class liquid methane engines has been developed for launching nanosatellites efficiently. This pump has to be operated at very low specific speed because it must be operated at very low flow rate, higher head, and higher rotational speed than conventional pumps. Therefore, this study focused on designing the impeller shape that can be operated while minimizing cavitation in very low specific speed. Two impeller candidates were manufactured through the design process presented in this paper, and impeller balancing was performed in the 20,000 RPM range. The shroud was applied to prevent the impeller and the casing from colliding. And it also minimizes the loss caused by recirculation. A volute casing with a circular cross-section is applied, and a brushless DC motor is used as a driver. Since the output of about 6 kW is required, an electronic speed controller is applied to control the motor and to supply power. Since the pump must be used in rocket engines, all the

components are contained in the smallest possible space. The bearings are arranged in a row with angular contact bearings that can withstand both axial and radial loads simultaneously. Also, instead of mechanical seals, simple spring-loaded seals were applied. Finally, all materials were selected in consideration of the cryogenic environment.

Keyword: Electric Pump, Cavitation, Specific Speed, Net Positive Suction Head, Net Positive Suction Head Required, Impeller, Low Cost

Student Number: 2018-23726

Contents

List of Tables

List of Figures

Nomenclature

ISP	specific impulse
RPM	*rotating per minute*
GPM	*gallon per minute*
Q	*volumetric flow rate*
$NPSH_{re}$	*net positive suction head required*
$NPSH_a$	*net positive suction head available*
t	*blade thickness*
Z	*blade number*
σ_c	Thoma cavitation coefficient
C_m	*absolute radial speed*
N_{ss}	*suction specific speed*
Ψ	*head coefficient*
η_v	*volumetric efficiency*
η_h	*hydraulic efficiency*
η_m	*mechanical efficiency*
η	*overall efficiency*
β_1	impeller inlet angle
β_2	impeller outlet angle
Ω	angular velocity
Φ	*inlet flow coefficient*

Chapter 1. INTRODUCTION

1.1 Background

Through the 4th Industrial Revolution, super-intelligence and hyper-connectivity realized, which allowed production and optimization of products simultaneously through CPS (Cyber-Physical System). And, with 3D printing technology, mass production and miniaturization of satellites are continuously made. So the demand for small satellites is expected to increase continually to realize global hyper-connection.

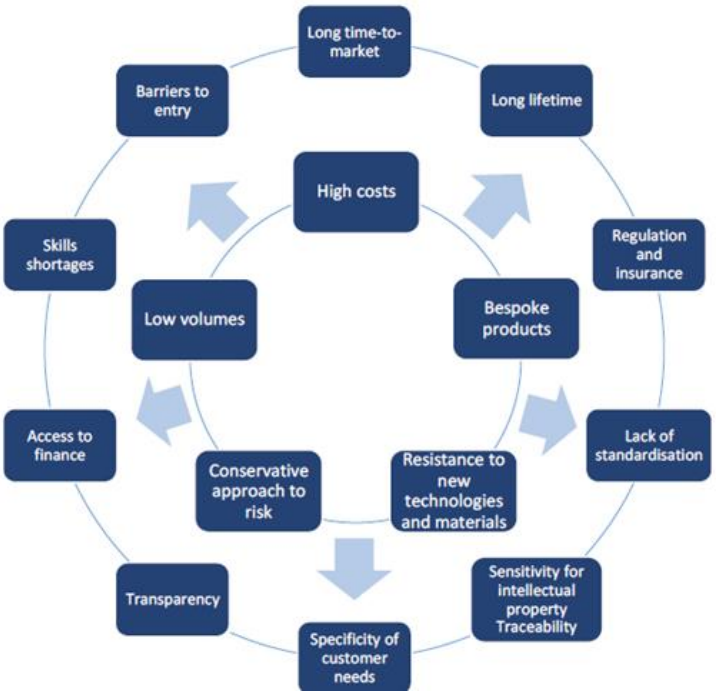

Fig 1.1 Industry 4.0 Technology

Through this Fourth Industrial Revolution, significant five barriers of space industries have broken down: high cost, low volumes, bespoke products, conservative approach to risk, resistance to new technologies and materials. As a result, the commercial potential of the aerospace industry has become visible, and the New Space era is coming where the initiative of the aerospace industry is shifting from the state to the private sector.

Looking at the trend of the New Space era, it can be seen as mass production, reusable engine, and miniaturization by the introduction of the fourth industrial revolution technology. Therefore, since the miniaturization of satellites will continue and the small space launch vehicle can be competitive in any country, this study focused on the miniaturization of the small space launch vehicle.

One of the notable features of developing such a small launch vehicle is that the engines with simple system configuration with electric pumps and batteries. Companies such as Rocket Lab are using these electric pump-fed engines instead of engines using turbines and gas generators.

With this in mind, the electric pump was seen as a trend to lead the small launch vehicle industry, and through this study, the electric pump for the small launch vehicle developed.

1.2 Overview of previous works

Electric pump cycles are simple to configure and easy to operate. Still, their limitations are clear, so you should analyze the pros and cons and run them in an advantageous operating range.

First of all, there are three significant advantages to the electric pump cycle. First, the ignition process is simplified, as shown in Fig. 1.2 [2]. This ease of reignition would be beneficial for reusable rockets and extraterrestrial probes.

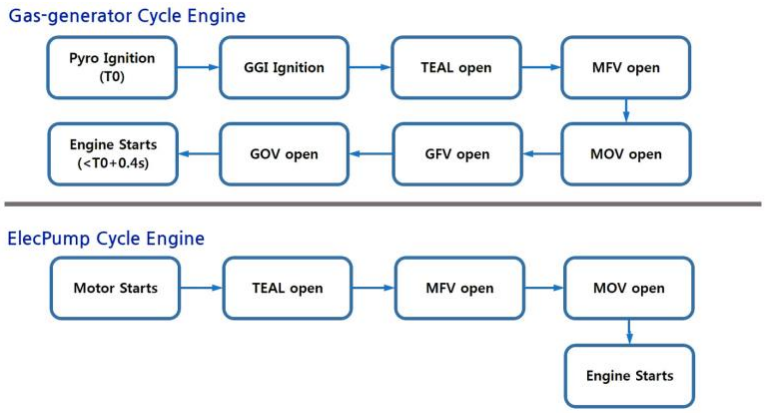

Fig 1.2 Ignition Sequence Comparison [2]

Second, compared to gas generator cycles, system configuration is simple since the pipe and valve components reduced, and the turbine vent is not required. Third, since there is no turbine and pre-burner, the combustion chamber is the only high-temperature part in the electric pump cycle, so it is easy to develop and operate.

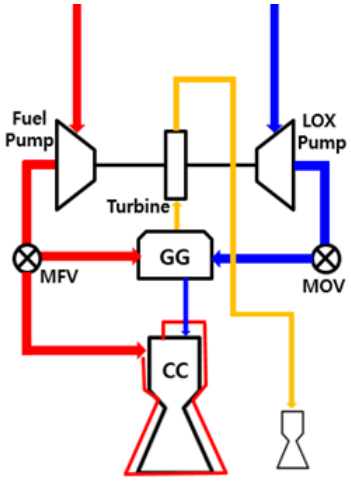

Fig 1.3 Gas Generator Cycle

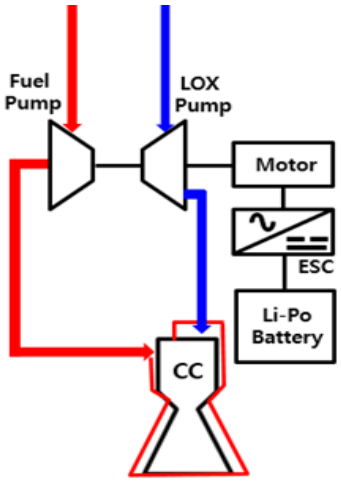

Fig 1.4 Electric Pump-fed Cycle

Next, the operable range of the electric pump cycle can infer using the fact that the thrust of the rocket engine is directly related to the output of the pump. That is, the maximum possible output of the electric pump cycle can derive by comparing the output range of the motor currently applicable to the small launch vehicle with the turbopump output of the existing rocket engine [2, 3]. In Fig. 1.5, a conventional turbopump cycle engine corresponding to the RPM and output of a motor can find in Fig. 1.6, which shows the maximum possible thrust of an engine using an electric pump cycle of about 100 kN.

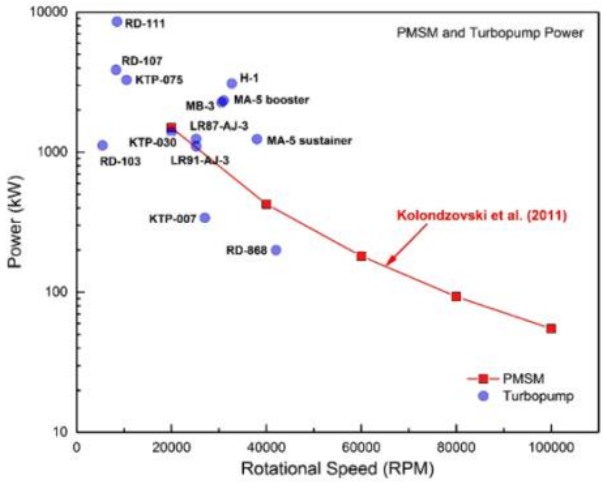

Fig 1.5 Rotational speed vs. turbopump power for PMSM power limits

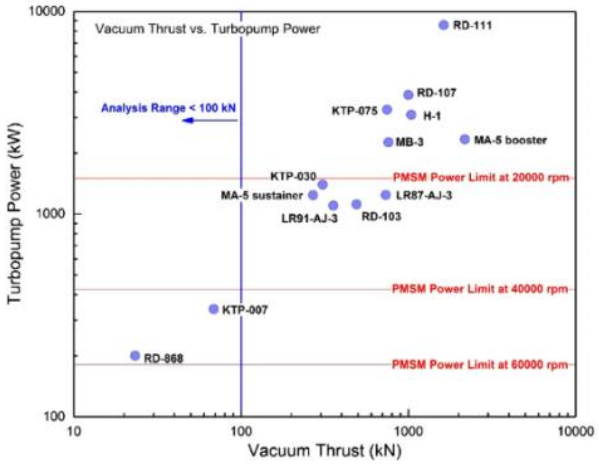

Fig 1.6 Vacuum thrust vs. turbopump power for PMSM power limits

As such, the electric pump cycle can apply to a thrust of about 10 tons or less. However, unlike the gas generator cycle in which all the turbine driving fuel discharges after the end of combustion, in the case of the electric pump cycle, the weight of the battery for driving the pump remains even after the end of combustion. This is a limitation of the electric pump cycle [2]. Therefore, it cannot apply to a rocket engine of 10 tons or less.

Kwak et al. Compared and analyzed the data of 3rd -stage engine of KSLV-II, which uses the gas generator cycle and the assumption of using the electric pump cycle in this engine. As a result, as shown in Fig. 1.7, when the combustion chamber pressure adequately lowered and the combustion time kept as long as possible, the performance of the electric pump cycle is close to the performance of the gas generator cycle engine.

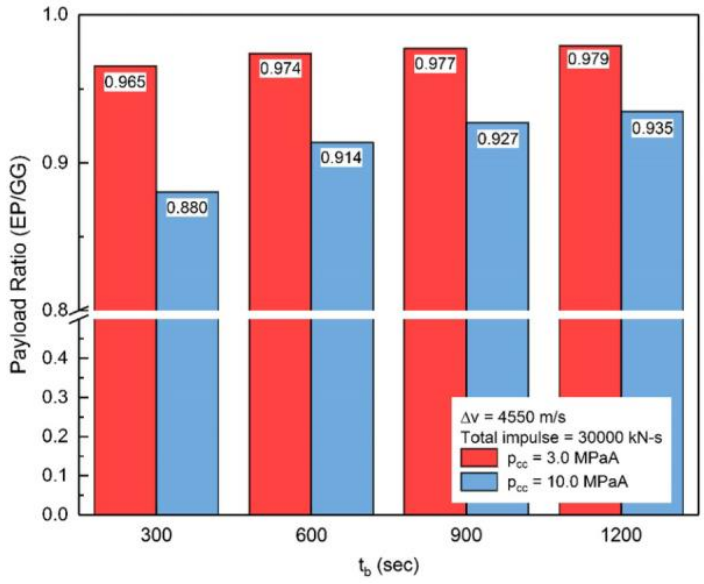

Fig 1.7 Payload Ratio of ElecPump Cycle to GG Cycle [2]

Also, the relationship between Battery Cell Energy Density and Payload Ratio compared with combustion chamber pressure, engine thrust, and combustion time as variables. The results show that the electric pump cycle engine can outperform the gas generator cycle engine when the combustion chamber pressure is 3.0 Mpa, and the combustion time is 700 seconds at 25 kN thrust, as shown in Fig. 1.8 [2].

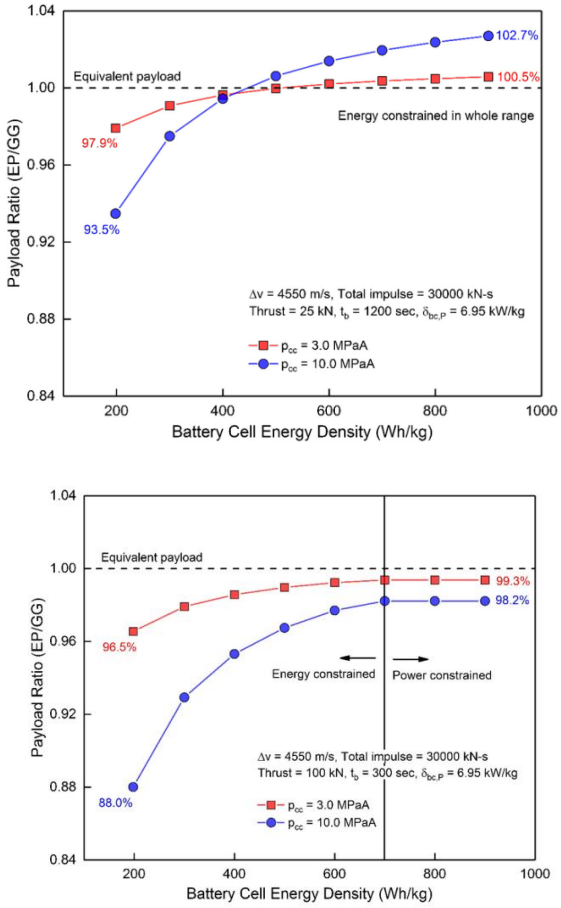

Fig 1.8 Payload Ratio of Elecpump Cycle to GG Cycle as a Function of the Battery Cell [2]

Therefore, if the electric pump cycle is applied only to the small low thrust rocket engine, the engine can perform better than the gas generator cycle with a short production period, easy QC, and low cost.

Indeed, all of the electric pump cycle engines that have been put to practical use or under development are for small engines of 10 tons or less.

Company	Thrust
Rocket Lab	37 kN
Bagaveev	10 kN
Astra Space	18 kN

Table 1.1 Current Status of Electric Pump Development by Various Companies

However, the trend of satellite launching shows a dramatic increase in the number of launches of small satellites, as shown in Fig 1.9. In particular, the increase in the ratio of nanosat among small satellites can see in Fig 1.10. Since the weight of the nanosat is less than 10kg, even a one-ton projectile can be inefficient for launching alone on the desired schedule unless ride-sharing or piggy back-fired.

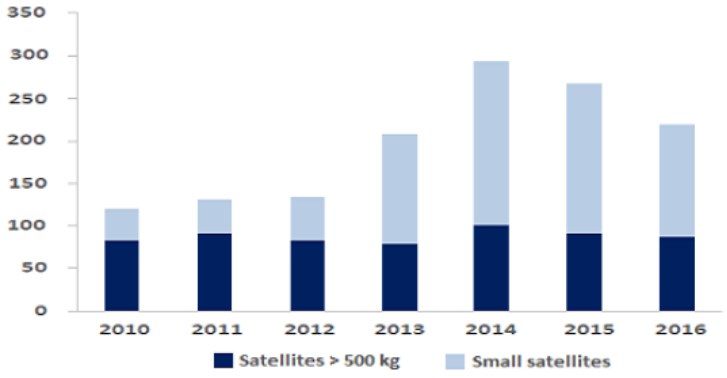

Fig 1.9 Historical Launches of Small and Large Satellites

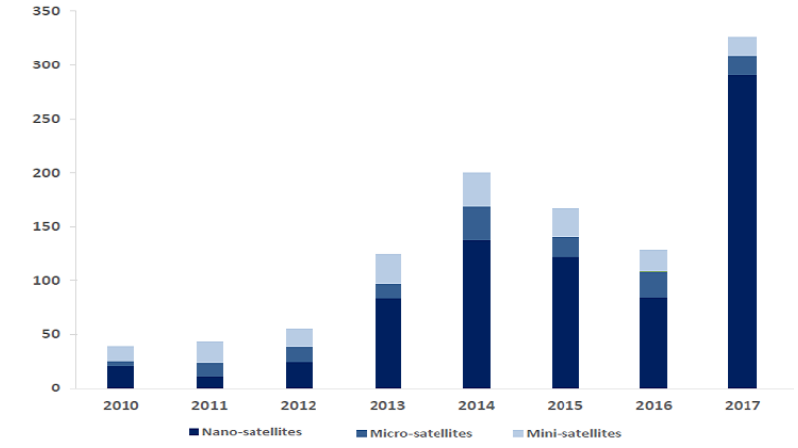

Notes: Satellite classification: Mini satellite: 100 kg – 500 kg; Micro satellite: 10 kg – 100 kg; Nano satellite: 1 kg – 10 kg.
Launch failures and other setbacks impacted the number of small satellites launched in 2015/16.

Fig 1.10 Historical Launches of Small Satellites by Type

1.3 Research Objectives

With the development of small launch vehicles, there is a movement to introduce electric pump cycles instead of gas generator cycles. However, as mentioned earlier, most electric pumps are for 1 ton or more engines. So, these are inefficient for launching a nanosat satellite of less than 10 kg.

Therefore, the purpose of this study is to develop an electric pump for a 5,000N class liquid methane engine for a launch vehicle that can launch nanosat satellites efficiently.

Through this, satellites, which are expecting to be further miniaturized in the future, can be efficiently launched alone, and low cost can be realized by enabling reusable engines using liquid methane.

However, the pump for the 5,000N class has a very low specific speed compared to the existing pumps, and at the same time, requires a high head, so a very high rotation speed is required to realize such performances.

Therefore, the purpose of this study is to design the impeller minimizing the cavitation and meet the requirements. Consequently, the electric pump was developed based on the impeller design through this study.

Chapter 2. PUMP DESIGN

2.1 Research Specification

The pump of this study was conducted based on the design conditions applied to the pintle combustor manufactured by rocket propulsion laboratory of Seoul National University.

Specifications applied to pintle combustors and electric pumps are shown in Table 2.1 and Table 2.2.

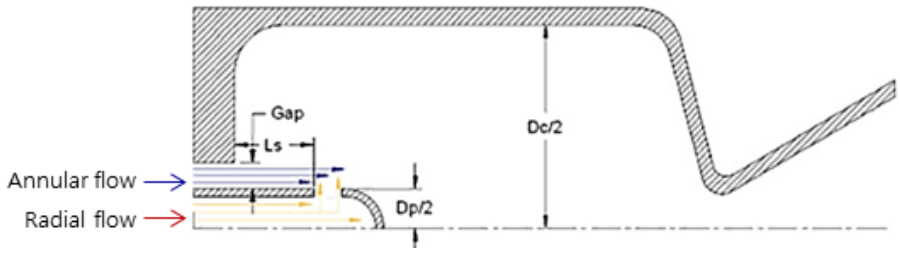

Fig 2.1 SNU Pintle Engine

	Value	Unit	Description
Fuel	CH4	-	-
Oxidizer	LOX	-	-
ISP	310	s	-
O/F Ratio	3.44	-	-
Mass Flow Rate	1.776	kg/s	-
Thrust	5395	N	-
Chamber P.	10	bar	-
Pressure Loss	8	bar	-

Table 2.1 Specification of SNU Pintle Engine

	Value	Unit	Description
Fluid	CH4	-	Liquid
Mass Flow Rate	0.4	kg/s	-
Density	442.4	kg/m3	-
Inlet Pressure	3	bar	-
Outlet Pressure	18	bar	-
Δ Pressure	15	bar	-
Δ Head	346	m	-
Angular Velocity	28,000	RPM	-

Table 2.2 Specification of Pump

The overall pump configuration is shown in Fig. 2.2.

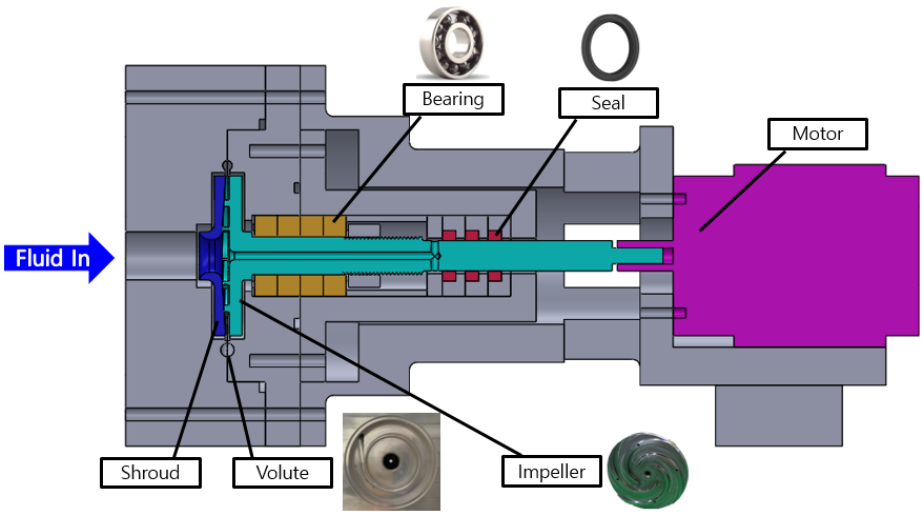

Fig 2.2 Pump Assembly

Since the aim is to handle cryogenic fluids and impeller rotates at very high speeds and are easy to ignite, a shroud is adopted to prevent friction between the impeller and volute casing and to reduce volumetric losses. And ceramic ball bearings that can operate in cryogenic fluids are applied. Also, the spring-loaded seals are used instead of mechanical seals for low cost and simple structures.

2.2 Impeller Design

As mentioned above, this study focused on the impeller design. The impeller is a device that raises the dynamic pressure by supplying kinetic energy to the fluid through the rotation. And the fluid passing through the impeller passes through the Volute Casing, and then the dynamic pressure is converted to static pressure and then discharged to the pump outlet.

As shown in Fig. 2.3, the impeller rotates at high speed, and the fluid entering the inlet passes through the impeller's vanes as a flow path and receives kinetic energy from the rotating impeller. The fluid passing through the impeller blades decelerated through the volute casing, and the dynamic pressure changed to static pressure. Therefore, to achieve the desired pump performance, it is necessary to design an impeller having a blade shape that can transfer energy well to the fluid without cavitation.

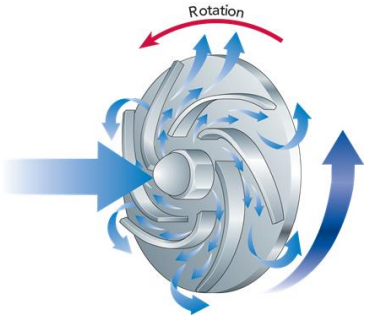

Fig 2.3 Pump Impeller [4]

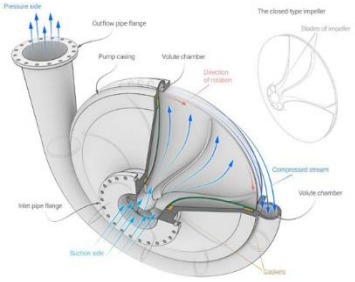

Fig 2.4 Volute Casing [4]

In this study, the impeller design was carried out according to Fig. 2.5.

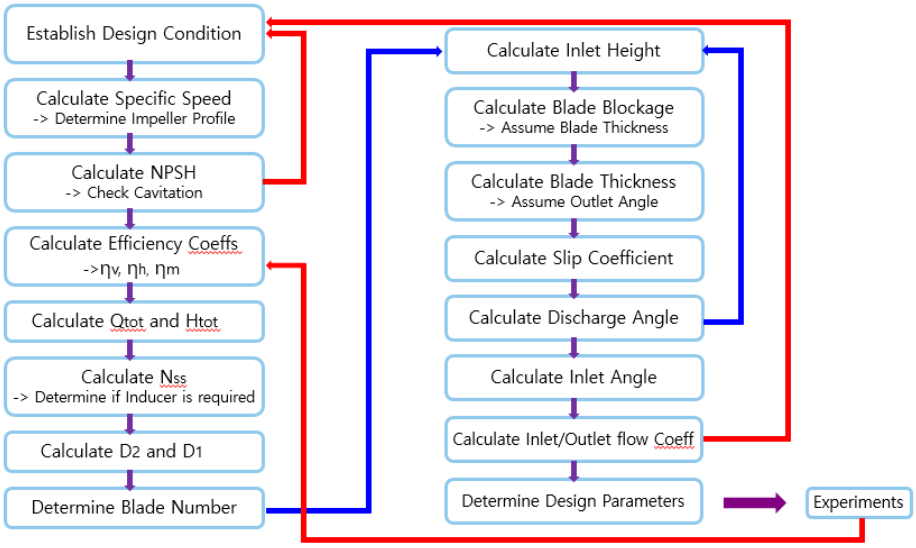

Fig 2.5 Impeller Design Process

Firstly, the Design Condition is as shown in Table 2.2. Based on Table 2.2, the specific speed is calculated.

$$N_s = RPM \times \frac{\sqrt{Volume\ flow\ rate}}{Head^{0.75}} = 540\ \text{(U.S. Units)}$$

Therefore, Radial Impeller was applied to this pump from Fig 2.6.

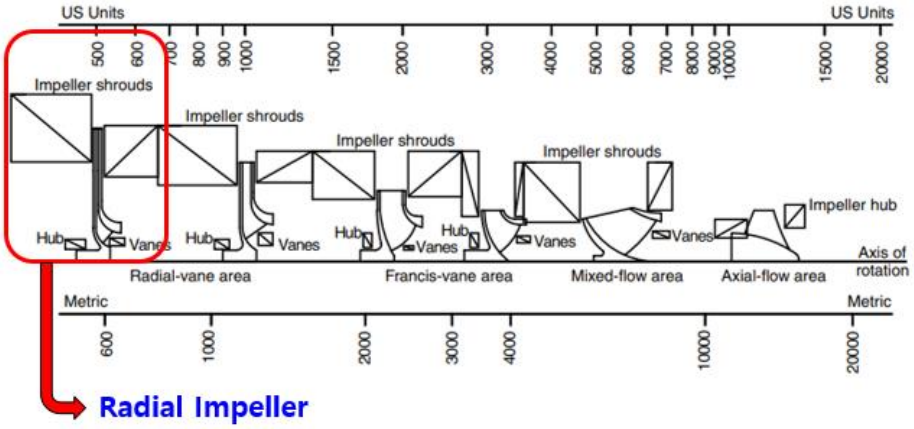

Fig 2.6 General Impeller Types [5]

Next, NPSHre (Net Positive Suction Head Required) was calculated to determine the possibility of cavitation. NPSHre is a value that can only be obtained as a result of the experiment after manufacturing the pump. So, the possibility of cavitation before manufacturing is evaluated based on the empirical formula presented by Shepherd and Stepanoff. At first, the theoretical definition of Thoma Cavitation number is as follows.

$$\text{Thoma Cavitation Coefficient} : \sigma_c = \frac{NPSHre}{Head}$$

The empirical Thoma cavitation numbers calculated by Shpherd and Stepanoff are as follows.

$$\sigma_c = \frac{N_s^{0.75}}{825} = 0.027853 \text{ [6] (SI Unit)}$$

$$\sigma_c = \frac{6.3 \times N_s^{0.75}}{10^6} = 0.027842 \text{ [7] (for single suction, US Unit)}$$

The NPSHre values expected from the above results and the definition of Thoma Cavitation numbers are as follows.

$$\mathrm{NPSH_{re}} = \sigma \times Head \cong 10\,m$$

Since the inlet pressure of this pump is 3 bar, NPSHa (Net Positive Suction Head available) values are as follows:

$$\mathrm{NPSH_a} = \frac{\text{Pressure}}{LCH_4\ density \times g} = 61 \text{ m}$$

Therefore, since NPSHa> NPSHre, it can be considered that the conditions of cavitation are not satisfied. Therefore, since NPSHa> NPSHre, it can be considered that the conditions for cavitation are not satisfied. So, the production was carried out according to the conditions in Table 2.2.

Next, the efficiency factors were examined. The efficiency factors should be obtained experimentally as well as NPSH, but firstly, the empirical equations and data known in the literature were applied to the conditions of Table 2.2, and then the validity of the design was examined.

There are three efficiency coefficients of the pump: volumetric efficiency,

hydraulic efficiency, and mechanical efficiency. The product of these three values is called the overall efficiency, which represents the overall efficiency of the pump.

First of all, the volumetric efficiency is shown in Table 2.3.

Description	Value
Karassik [8]	0.21
Huzel [9]	0.01~0.05
Fig 2.7, Fig 2.8 [10], [12]	0.15

Table 2.3 Volumetric Efficiency

$$\eta_v = 5 \cdot \left[\frac{\frac{\delta}{r_R} \cdot \left(\frac{r_e}{r_2}\right)^2}{n_s^2 \cdot \Psi} \right] = 0.21 \quad [8], \text{ Karassik}$$

$\frac{\delta}{r_R}$: Clearance Ratio, $\frac{r_e}{r_2}$: Eye to tip Ratio

n_s : Specific Speed, Ψ : Head Coefficient

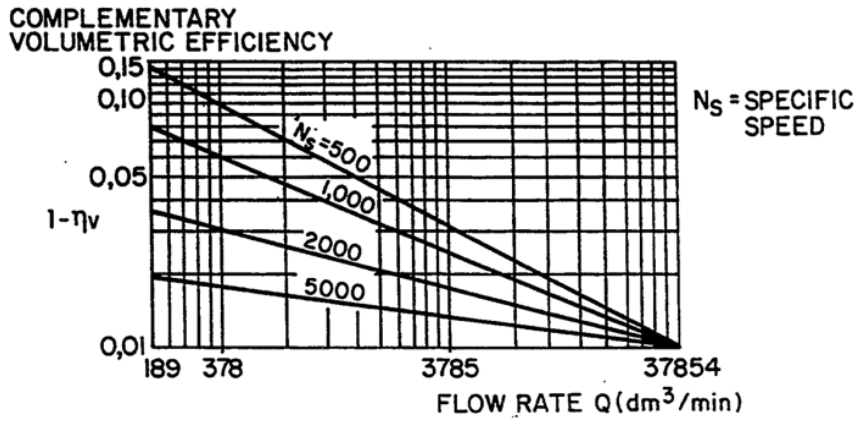

Fig 2.7 Volumetric Efficiency vs. GPM [10]

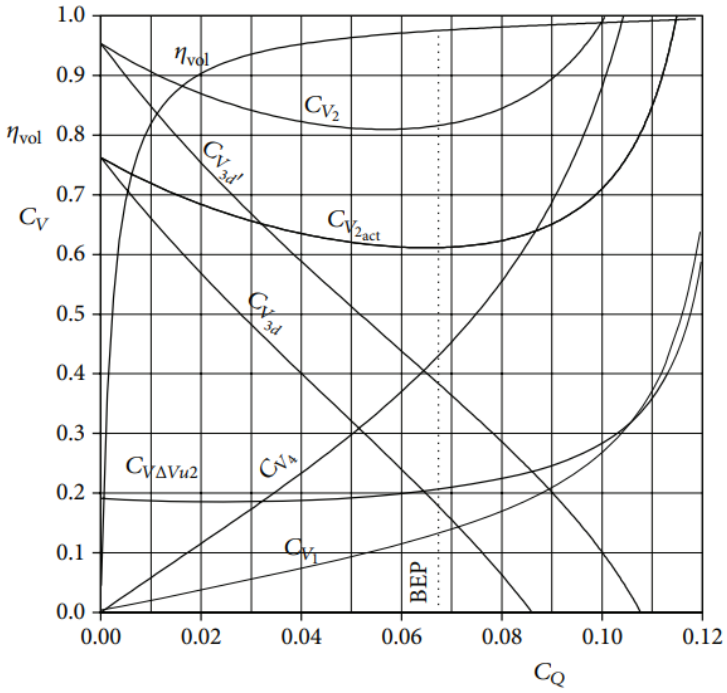

Fig 2.8 Values of Volumetric Efficiency and Velocity Coefficients [12]

In the above results, assuming that the pump is a small pump with a low flow rate and high head, the recommended value by Huzel is too small. And Karassik's empirical value is inadequate for the small pump. So, The initial volumetric efficiency is assumed to be 15% based on Fig 2.7 and Fig 2.8.

Next, the hydraulic coefficients are shown in Table 2.4.

Description	Value
Karassik [8]	0.6
Huzel [9]	0.7~0.9
Gulich [11]	0.5

Table 2.4 Hydraulic Efficiency

$$\eta_h = 1 - \frac{0.071}{Q^{0.25}} = 0.6 \qquad [8]\ \text{(SI Unit)}$$

$$\eta_h = 1 - 0.055 \cdot \left(\frac{Q_{Ref}}{Q}\right)^m - 0.2 \cdot \left(0.26 - \log\frac{n_q}{25}\right)^2 \left(\frac{Q_{Ref}}{Q}\right)^{0.1} = 0.5 \quad [11]\ \text{(SI Unit)}$$

In the above results, considering that this small pump has a high head and low flow rate pump, the value by Huzel is deemed to be too large, and the value by Gulich is too small. Therefore, 0.6 by Karassik is selected as the hydraulic efficiency value.

The mechanical efficiency applied to the following values. In this case, the overall efficiency was calculated from the initial assumption and then corrected through iterative calculation.

$$\eta_m = 1 - \frac{\frac{C_m \cdot \eta}{2}}{n_s^2 \cdot \Psi^{2.5}} = 0.84\ ,\ C_m = 0.004\ ,\ \eta = \text{overall efficiency} \quad [8]$$

The overall efficiency value is as follows

$$\eta = \eta_v \eta_h \eta_m = 0.43$$

Therefore, the estimated efficiency of the pump, which was calculated through the above calculation, is about 43%. In order to examine the validity, the overall efficiency can be calculated using empirical equations by Karassik [8].

$$\eta = 0.94 - 0.08955 \times \left[\frac{Q(\text{gpm})}{N(\text{rpm})} \times X\right]^{-0.21333} - 0.29 \times \left[\log_{10}\left(\frac{2286}{N_s}\right)\right]^2 = 0.49$$

$$X = \left[\frac{140}{\varepsilon(\mu\text{-in.})}\right] \qquad \varepsilon : \textit{surface roughness height SUS} : 24\,\mu - in$$

In addition, if you look at the area of the pump in Fig. 2.9, it is also 40% - 50%, so the above calculation results can be considered as valid.

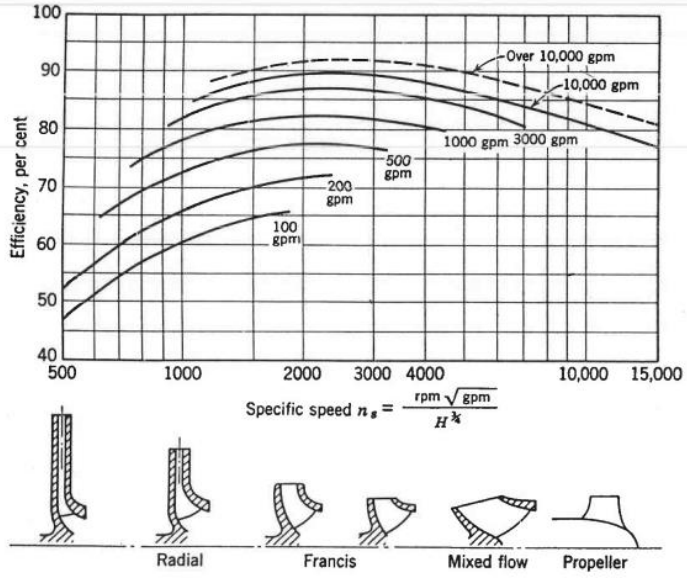

Fig 2.9 Pump Efficiency vs. Specific Speed and Pump Size [7]

Based on these efficiency factors, the actual pump operating conditions to satisfy the required performances of Table 2.2 were determined as shown in Table 2.5.

	Value	Unit	Description
ΔH	346	m	Design Head
Q	0.0009	m^3/s	Total Volumetric Flow
ΔH_t	484	m	Design Head
Q_t	0.00104	m^3/s	Total Volumetric Flow

Table 2.5 Design Criteria

Next, the inlet flow coefficient and suction specific speed were calculated to determine whether the inducer is needed or not.

$$\phi_{inlet} = \frac{cm_1}{U_1} = 0.3 > 0.2$$

In Figure 2.10, we can see that Brumfield's criteria value grows rapidly when the flow coefficient is lower than 0.2.

Brumfield's criteria is a line that collects the maximum points of suction specific speed for several cavitation coefficients. Therefore, if the flow coefficient is larger than 0.2, it can be seen that the inducer does not need to be applied.

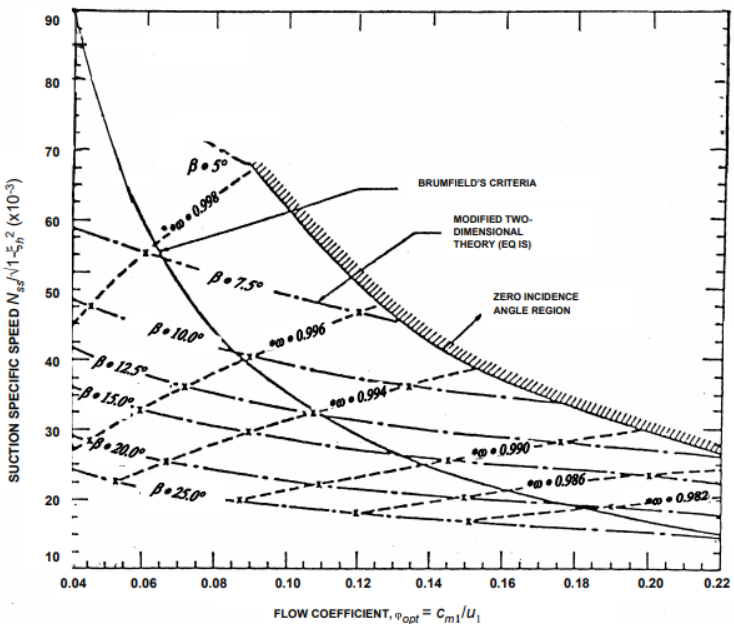

Fig 2.10 Suction Specific Speed vs. Optimum Flow Coefficient

Also, it is possible to determine the necessity of the inducer through the suction specific speed evaluation. In this study, the suction specific speed is about 3600, and the value is smaller than 10,000 [7]. Therefore, the inducer was not applied to the pump.

$$N_{ss} = \frac{RPM \cdot \sqrt{Q_{tot}}}{NPSHre_{tot}^{0.75}} = 3569 < 10{,}000$$

From the above results, it can be seen that in the case of small pumps with low flow rates and high head, the low circumferential speed produces a large

inlet flow coefficient. And the large head and the small volume flow rates tend to have a lower suction specific speed. It demonstrates the possibility of making hydraulic calculations easier and advantageous in size and weight by adjusting the design parameters well so that the inducer is not applied in the development of low thrust small engines.

Next, the outer and inner diameters of the impeller disk were calculated. The impeller outlet diameter is mainly determined by the head coefficient, which is also needed to be determined experimentally. So, in the initial production stage, the head coefficient was first set to 0.55 [14].

	Humble [14]	Gulich(I) [11]	Guilich(II) [11]
Outlet Diameter (mm)	63.3886	63.4023	64.9879

Table 2.6 Impeller Outlet Diameter

$$D_{outlet} = \sqrt{\frac{g \cdot H}{\Psi_{humble} \cdot N^2}} = 63.3886 \quad [14]$$

$$D_{outlet} = \frac{84.6}{n} \cdot \sqrt{\frac{H_{opt}}{\Psi_{humble}}} = 64.4023 \quad [11]\ \text{Guilich (I)}$$

$$D_{outlet} = \frac{84.6}{n} \cdot \sqrt{\frac{H_{opt}}{1.12 \cdot e^{-0.408 \cdot n_s}}} = 64.9879 \quad [11]\ \text{Guilich(II)}$$

In order to verify the validity of this value, the outlet diameter is calculated as below with Bernoulli's equation by assuming that the required head and

increasing dynamic pressure are the same.

$$H_{tot} \cdot \rho \cdot g = 0.5 \cdot U_2^2 \qquad U_2 = 97.4\ m/s \qquad U_2 = \left(\frac{D}{2}\right) \cdot \omega \quad \rightarrow \quad D_{outlet} = 66.4\ mm$$

Considering the loss value, the actual circumferential velocity will be slower, so it seems the outlet diameter value derived above is reasonable. Therefore, in this study, the outlet diameter of the impeller was determined to be 63mm.

Inlet Diameter was derived from Huble's equation [14]. However, since the purpose of this study is low cost, 19mm was adopted to apply a 3/4 inch pipe, which is widely used in industry, rather than 16.5mm calculated by Humble's equation. In practice, if the diameter ratio (D_2 / D_1) is less than 0.7 [14], it does not matter [14], and as the diameter ratio is larger in this range, the stability of the pump tends to increase [15].

$$D_1 = \left(\frac{4Q}{\pi(1 - L^2)\Omega}\right)^{\frac{1}{3}} = 16.5\,mm \quad [14]$$

Four blades were used. As the volute type, single volute was adopted as shown in Fig 2.11. Due to the small size and low flow rate, the radial thrust acting along the impeller radius is small, so there is no need to adopt double volute or more. And there is no need to select an odd number of blades; the number of blades was set to four to reduce space efficiency and weight in the pump.

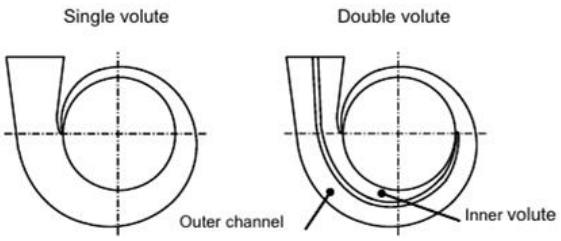

Fig 2.11 Single and Double Volute

The thickness of a blade, which is made of SUS304, was calculated to be 0.9 mm to withstand the circumferential speed of 92 m/s and about 10 degrees of discharge angle at the impeller outlet. However, since the connection between shroud and impeller was made using M2 bolts, 2.5mm was adopted for this purpose.

For the other impeller with a discharge angle of 32 degrees to be mentioned later, the required thickness is about 2.8mm. However, the inlet thickness is made relatively thin due to the slow circumferential speed, and the outlet thickness is made as thick as necessary to endure high circumferential speed and large discharge angle. In this way, weight can be reduced. The blade parameters determined using this thickness value as blade blockage are shown in Table 2.7.

	Value	Unit
Blade Number	4	-
Blade Thickness	2.5	mm
Blade Inlet Height	2.9	mm
Blade Tip Height	1.5	mm

Table 2.7 Blade Parameters

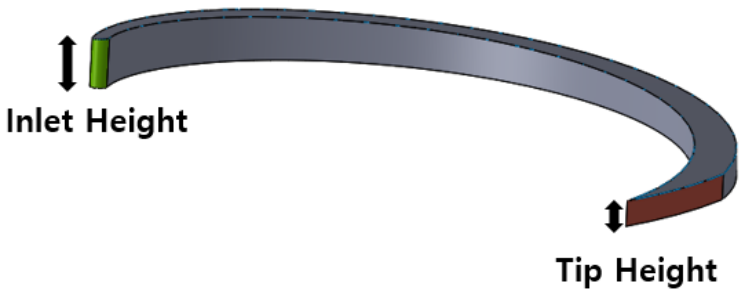

Fig 2.12 Impeller Blade

Finally, the inlet / outlet blade angle was obtained using the velocity triangle shown in Fig. 2.13 to determine the impeller shape. Since inducer was not adopted, the inlet was considered to have no pre-rotation, and the circumferential velocity of the impeller was calculated as C_{1u}. The angle exaggeration considering hydraulic loss was applied 15%. In the case of the outlet, C_{2u} was derived from Euler's turbomachinery equation [9]. Unlike the inlet, since the fluid receives the rotational energy by the impeller, pre-rotation exists. So, the slip factor [16] is considered to the velocity triangle.

$$\Delta H = \frac{C_{2u} \cdot U_2 - C_{1u} \cdot U_1}{g} \quad \text{Euler's Turbomachinery eqn.}$$

$$\varepsilon = \frac{1}{1 + \frac{0.5 \cdot \pi \cdot \sin(\beta_2)}{z \cdot (1 - \delta)}} \quad \text{Slip Coefficient}$$

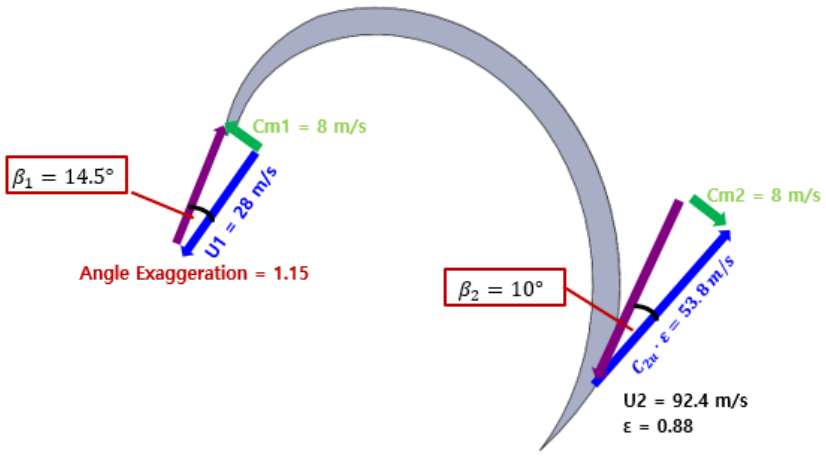

Fig 2.13 Velocity Triangle

In order to check the validity of the values from the velocity triangle, the inlet/outlet flow coefficient is as follows.

$$\phi_{inlet} = \frac{cm_1}{U_1} = 0.3 \quad \rightarrow \quad 0.05 < 0.3 < 0.4$$

$$\phi_{outlet} = \frac{cm_2}{U_2} = 0.1 \quad \rightarrow \quad 0.05 < 0.1 < 0.8$$

Since these values are all within the range of the existing recommended values [8, 9, 14], the design variables are confirmed, as shown in Table 2.8.

	Value	Unit	Description
D_1	19	mm	inlet diameter
D_2	63	mm	outlet diameter
β'_1	14.5	deg	inlet angle
β'_2	10	deg	outlet angle
t	2.5	mm	blade thickness
Z	4	-	blade number

Table 2.8 Final Design Parameters

However, in the above values, the discharge angle of 10 degrees is significantly smaller than the recommended range given in Table 2.9. Therefore, the validity of this small discharge angle needs to be examined.

	Huzel [9]	Gulich [11]
Recommended outlet angle	$17^\circ < \beta_2 < 40^\circ$	$15^\circ < \beta_2 < 45^\circ$

Table 2.9 Recommended Outlet Angle

The correlation between the impeller discharge angle and pump performance is shown in Fig 2.14 that the larger the discharge angle, the higher the performance of the head. Also, from Fig 2.15, it is known that hydraulic efficiency tends to show an abnormal tendency around the design point when the discharge angle exceeds 35 degrees [17].

In summary, the higher the discharge angle is advantageous to derive the head performance, but the excessively high discharge angle is disadvantageous to take a wide operating range due to the falling stability.

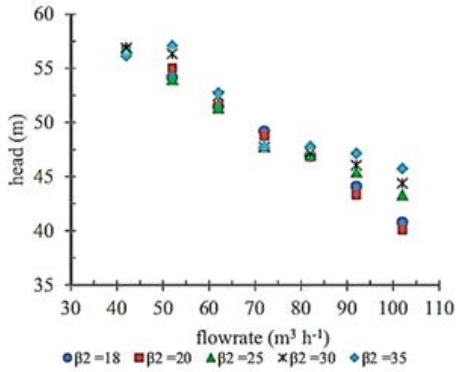

Fig 2.14 Exit Blade Angle vs. Head [17]

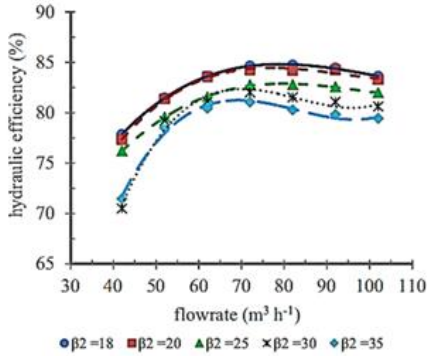

Fig 2.15 Exit Blade Angle vs. Hydraulic Efficiency [17]

Besides, it can be seen from Fig 2.16 that long flow paths are advantageous to achieve stable performance in the 3000rpm region under very low specific speeds of 10 or less in SI unit standard [15].

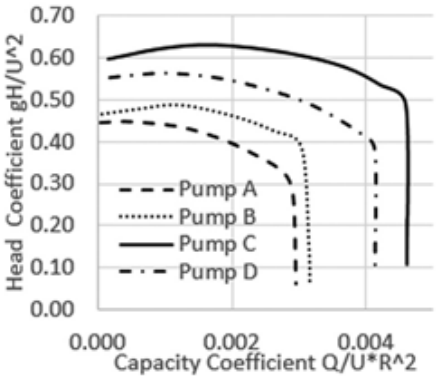

Fig 2.16 Head Coefficient of Various Impellers

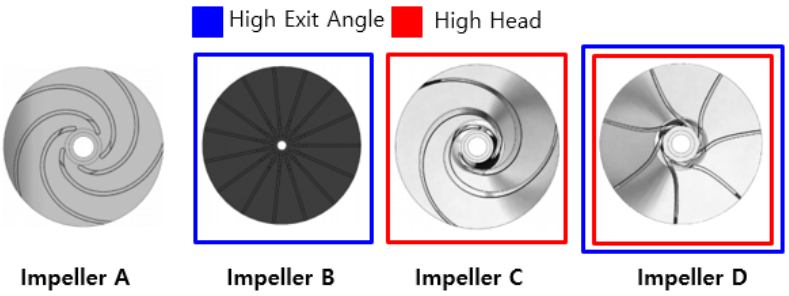

Fig 2.17 Various Types of Impeller for Very Low Specific Speed [15]

In terms of the shape of the impeller, the high discharge angle like the impeller D from Fig 2.17 can improve the head performance, but the stability is inferior from the slope shown in Fig 2.16. And, since this pump is a very high-speed pump close to 30,000 rpm and the forward blade shape seems to strain the impeller, only the backward blade shape was considered. For small discharge angles when long flow paths are adopted, such as Type C, it is possible to secure both head performance and stability as it can be seen from Fig 2.16.

The pump to be made in this study is a model that operates at high rotational speed with a low specific velocity between 8 and 10 based on SI unit system. Therefore, β'1 applies the values in Table 2.8 so that the inlet can be a shockless inlet to minimize the effects of cavitation. For outlet angles and blade geometries, two types of impellers were manufactured. One is an impeller with long flow paths, as shown in Fig 2.18 and with discharge angles β'2 in table 2.8. And the other is an impeller with traditional geometry such as impeller A in Fig 2.17 and with a discharge angle of 33 degrees, which is within the recommended value range of table 2.9. Through experiments, the two types of impellers will be compared to find the proper impeller shape for the small high-speed pump which has low specific speed.

Fig 2.18 Long Flow Path Impeller

Fig 2.19 High Exit Angle Impeller

2.3 Volute Design

The volute cross-section usually adopts one of the shapes shown in Fig 2.20. Although the trapezoidal or rectangular cross-section is generally advantageous in terms of production time and cost, since a high head, low flow rates are required in this study, so the circular shape is applied for more stable flow.

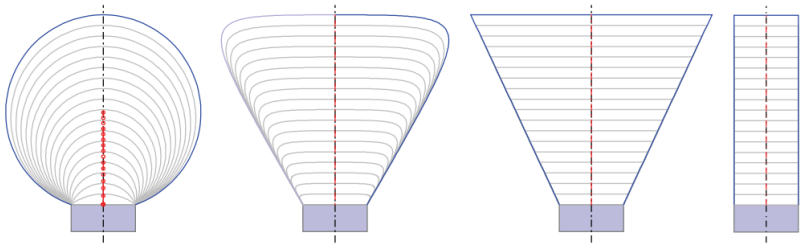

Fig 2.20 Four Types of Cross-Sectional Shapes [18]

Also, since the dissipation loss is expected to be small because it is a small pump, it is manufactured by applying the symmetric volute shape instead of the folded volute.

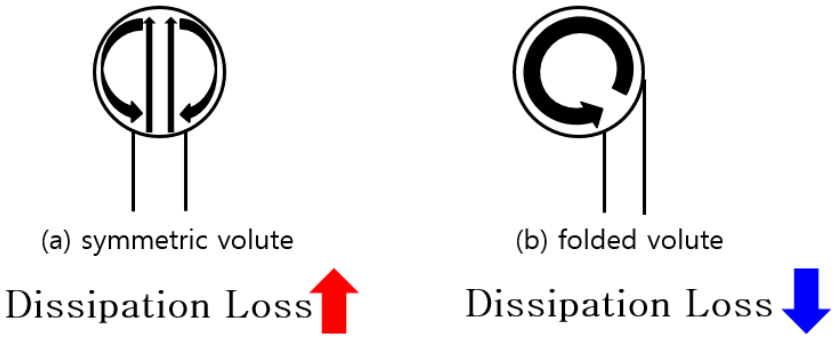

Fig 2.21 Symmetric Volute and Folded Volute

The volute design of this pump with symmetric volute configuration is shown in Fig 2.22.

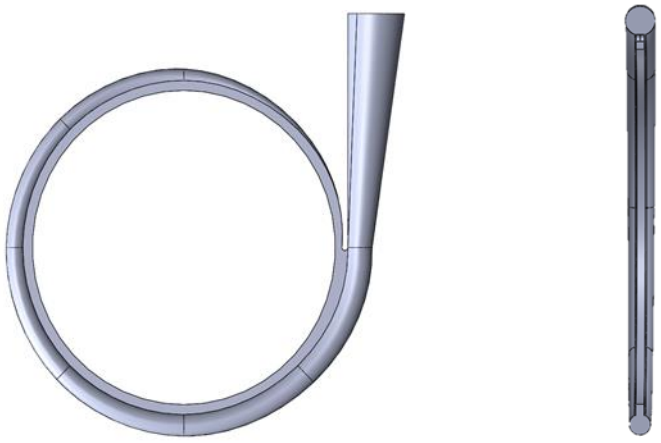

Fig 2.22 Plan View and Meridional View of Volute

Chapter 3. RESULTS

Impellers manufactured according to the shapes shown in Fig 2.18 and Fig 2.19 are shown in Fig 3.1 and Fig 3.2, respectively. In addition, the impeller and shroud are combined as shown in Fig. 3.3, and the volute is manufactured as shown in Fig. 3.4. Four rangular contact ball bearings which can withstand axial thrust and radial thrust from the differential pressure in the casing. And these bearings are made of ceramic materials to withstand the cryogenic environment. The final assembly is shown in Fig. 2.2.

Fig 3.1 Long Flow Path Impeller

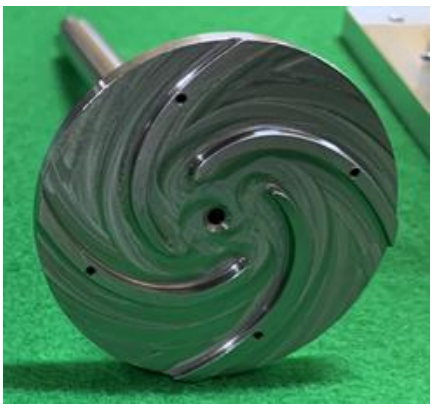

Fig 3.2 High Exit Angle Impeller

Fig 3.3 Shrouded Impeller

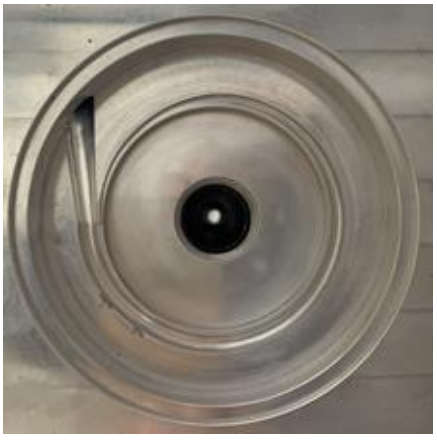

Fig 3.4 Volute Casing

Chapter 4. CONCLUSION

Through this study, an electric pump for liquid methane for 5,000N class methane engine was designed and manufactured. Since the purpose of this study was to realize low cost, the manufacturing cost was calculated, and it cost about 6 million won except for the battery.

However, this pump is just a prototype and manufactured with safety as the top priority. As a result, the casing and various parts except the impeller were made excessively thick. And unlike the existing companies operating the pump in the 40,000 RPM region, this pump was manufactured to operate in the 28,000 RPM region, so the diameter of the impeller was inevitably large.

So, there is a lot of room for cost and weight reduction if optimization is performed based on the data obtained through future experiments and if higher rotation speed and 3D printing technology are applied. Through this, it will be possible to develop a pressurization system that is more efficient and lower cost than the existing turbopump system.

In the future, the head and efficiency will be measured using a device such as Fig. 4.1, and the stability of the pump and NPSH will be tested. And then data from experiments will be used to develop more efficient small pump impellers by improving the impeller shape and applying the measured efficiency factor to the design process of Fig 2.5.

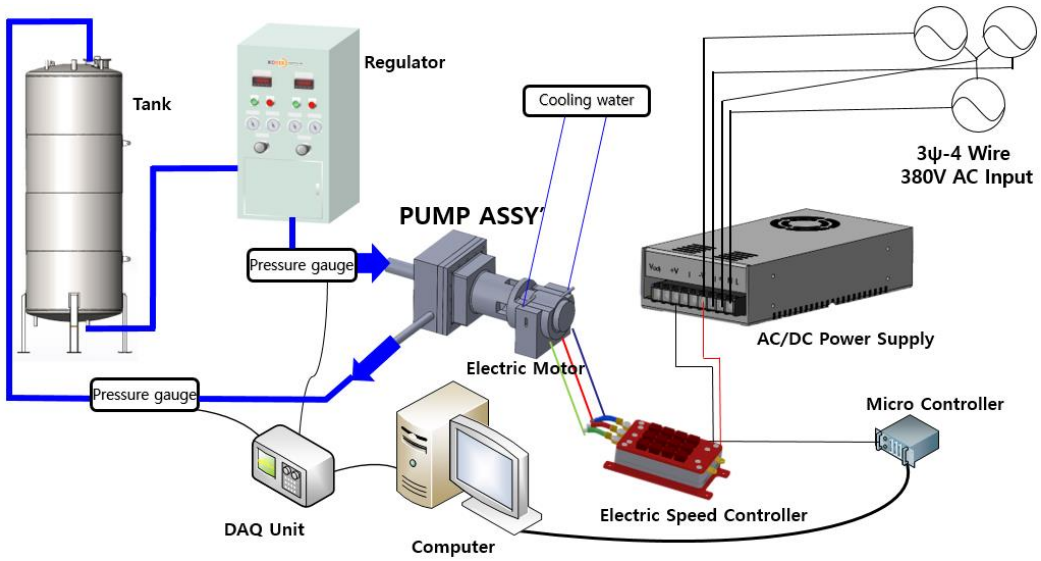

Fig 4.1 Experimental Setup

Bibliography

[1] London Economics, “Industry 4.0 and the Future of UK Space Manufacturing, 2019

[2] H. D. Kwak, S. J. Kwon, C. H. Choi, “Performance assessment of electrically driven pump-fed LOX/kerosene cycle rocket engine: Comparison with gas generator cycle, Aerospace Science and Technology, 2017

[3] Z. Kolondzovsk, A. Arkkio, J. Larjola, P. Sallinen,“Power limits of high-speed permanent-magnet electrical machines for compressor applications, IEEE Trans. Energt Convers. 26, 2011

[4] D. Parikh, Indroduction to Hydraulic Pumps, 2019

[5] Hydraulic Institute Inc, Parsippany, New Jersey

[6] Subramanya, Hydraulic Machines, McGRAW-HILL

[7] J. J. Stepanoff, Centrifugal and Axial Flow Pumps 2nd Edition, KRIEGER PUBLISHING COMPANY

[8] Igor J. Karassik, Joseph P. Messina, Paul Cooper, Charles C. Heald, Pump Handbook 3rd Edition, McGRAW-HILL

[9] D. K. Huzel, D. H. Huang, Modern Engineering for Design of Liquid Propellant Rocket Engines, AIAA

[10] J. R. Lehe, Andre Beaurain, Rene Bosson, Etienne Tiret, High Performance Centrifugal Pump Having An Open-Faced Impeller, U.S. Patent

[11] J. F. Gulich, Centrifugal Pumps 2nd Edition, Springer

[12] Mohammed Ahmed El-Naggar, A One-Dimensional Flow Analysis for the Predidction of Centrifugal Pump Performance Characteristics, International Journal of Rotating Machinery

[13] David Japikse, Overview of Industrial and Rocket Turbopump Inducer Design, CaltechCONF, 2001

[14] R. W. Humble, G. N. Henry, W. J. Larson, Space Propulsion Analysis and Design, McGRAU-HILL

[15] G. Olimstad, M. Osvoll, P. H. E. Finstad, Very Low Specific Speed Centrifugal Pump – Hydraulic Design and Physical Limitations, Jounal of Fluids Engineering, 2018

[16] Balje, Turbomachines: A Guide to Design, Selection and Theory, John Wiley & Sons

[17] O. Babayigit, O. Kocaaslan, M. Hilmi Aksoy, K. M. Guleren and M. Ozgoren, Numerical identification of blade exit angle effect on the performance for a multistage centrifugal pump impeller, EPJ Web of Conferences, 2015

[18] S. Yang, F. Kong, B. Chen, Research on Pump Volute Design Method Using CFD, IJRM, 2011

초 록

4차 산업혁명으로 인하여 소형위성의 수요가 크게 증가하고 있으며, 이러한 소형 위성을 효율적으로 발사하기 위한 소형 발사체 시장 역시 빠르게 성장하고 있다. 그러나 최근, 기존의 대형 발사체에 사용하고 터보펌프 시스템은 구성이 복잡하고 차지하는 공간이 크며 제작 및 운용비용마저 높아, 터보펌프 대신 저비용으로 소형발사체에 적용할 수 있는 대체제로써 전기펌프 시스템이 주목받고 있다. 특히 배터리 기술의 비약적인 발전으로 인하여 가볍고 에너지 밀도가 높은 배터리가 개발됨에 따라 소형 발사체에 한하여 터보펌프 대신 더욱 효율적이며 가격은 낮은 전기펌프 시스템을 적용하는 것이 가능해 지게 되었다. 그러나 근래의 소형 발사체는 대부분이 1톤급 이상의 추력을 갖는 발사체로써, 최근 급격히 증가하고 있는 나노위성을 단독발사 하기에는 적절치 않다. 따라서 본 연구를 통하여 나노위성을 효육적으로 단독발사 할 수 있는 5,000 뉴튼급 액체메탄 엔진 구동을 위한 액체메탄 전기펌프를 개발하였다. 이 펌프는 유량이 기존펌프 대비 매우 작으면서 높은 양정을 가지며 28,000 RPM의 상당히 높은 회전수를 갖기 때문에 매우 작은 비속도의 영역에서 운전되어야만 한다. 따라서 본 연구에서는 매우 작은 비속도 영역에서 케비테이션 발생을 최소화 하며 정상적으로 작동할 수 있는 임펠러 형상을 설계하는 것에 주안점을 두고 개발을 진행하였다.

본론에 제시된 설계과정을 통하여 두 가지의 임펠러 후보군을

제작하였고 20,000 RPM 영역에서 임펠러 바란싱을 수행하였으며 임펠러와 케이싱의 충돌을 방지하고 재순환으로 인한 손실을 최소화 하기 위하여 시라우드를 적용하였다. 케이싱으로는 원형 단면의 케이싱을 적용하였으며 구동 모터로는 브러시리스 직류 모터를 이용하였고 약 6kW의 출력이 필요하여 모터 제어 및 전력공급을 위한 모터 변속기를 추가로 장착하여 전기모터 시스템을 구축하였다. 본 펌프는 로켓 엔진 적용을 고려 했기 때문에 최대한 좁은 공간에 모든 구성품이 들어가도록 하기 위하여 축방향과 경방향 하중을 동시에 견딜 수 있는 앵귤러 컨택트 베어링을 채택하여 일렬로 배치하였으며 복잡하고 큰 미케니칼 씰을 대신하여 간단한 구조의 스프링 씰을 적용하였다. 마지막으로 모든 소재의 선정은 극저온 환경을 고려하여 진행하였다.

주요어: 전기펌프, 케비테이션, 비속도, 유효흡입수두, 최소흡입수두, 임펠러, 저비용

학 번: 2018-23726